AR-010-644

DSTO

Variational Bounds for the Equivalent Spring Constants for Bonded Repairs

Peter Chalkley and L.R.F. Rose

DSTO-RR-0139

APPROVED FOR PUBLIC RELEASE

© Commonwealth of Australia

DEPARTMENT ◆ OF DEFENCE

DEFENCE SCIENCE AND TECHNOLOGY ORGANISATION

Variational Bounds for the Equivalent Spring Constants for Bonded Repairs

Peter Chalkley and L.R.F. Rose

Airframes and Engines Division
Aeronautical and Maritime Research Laboratory

DSTO-RR-0139

ABSTRACT

Variational bounds, both upper and lower, are found for the equivalent spring constant of a double-strap joint which represents a sub-element of bonded repairs to cracked structure. Conservative estimates of the equivalent spring constant, needed for accurate design, are obtained from variational analyses of the joint. Estimates from various analytical models of varying level of approximation were obtained. Simpler expressions for the spring constant resulted from relaxing certain assumptions, however, the theoretical guarantee of a true upper or lower bound was lost. Spring constant estimates were compared with finite-element model results and so the fidelity of the variational bounds, specially for the simplified analyses, could be established. An improved formula is proposed for use in design procedures in RAAF C5033.

19990308191

RELEASE LIMITATION

Approved for public release

DEPARTMENT OF DEFENCE

DEFENCE SCIENCE AND TECHNOLOGY ORGANISATION

DTIC QUALITY INSPECTED 1

AQF 99-05-1116

Published by

DSTO Aeronautical and Maritime Research Laboratory
PO Box 4331
Melbourne Victoria 3001 Australia

Telephone: (03) 9626 7000
Fax: (03) 9626 7999
© Commonwealth of Australia 1998
AR-010-644
September 1998

APPROVED FOR PUBLIC RELEASE

Variational Bounds for the Equivalent Spring Constants for Bonded Repairs

Executive Summary

Bonded composite repairs are an effective and cost-efficient means of restoring the life of cracked metallic aircraft components. The Aeronautical and Maritime Research Laboratory (AMRL) has used this technique for over 25 years to repair damaged Royal Australian Air Force (RAAF) aircraft. A critical step in the repair design process is to obtain an accurate estimate of the stress-intensity factor associated with the crack in the metallic component after application of the repair. In the initial design stage, analytical formulae are used to obtain these estimates.

This report evaluates various analytical models (some developed by the authors) that can be used to obtain post-repair stress-intensity-factor estimates through the concept of equivalent spring constants. The bonded composite repair can be thought of as a series of springs resisting the opening of the underlying crack when a load is applied. The springs are characterised by a spring constant and the validity of the various models is explored through consideration of this constant. Of particular concern is that the models provide truly conservative estimates (an upper bound for the spring constant) that can reliably be used in the design process. For this reason, a complementary energy functional for the bonded repair was constructed with the use of either stress or displacement based potentials and a variational analysis undertaken to provide an upper or lower bound respectively.

The most suitable model for design purposes – one which provides conservative design estimates and is not too mathematically complex - was identified. This model will be proposed to the RAAF for inclusion in RAAF Engineering Standard C5033 – "Composite Materials and Adhesive Bonded Repairs".

Authors

Peter Chalkley
Airframes and Engines Division

Peter Chalkley is a Professional Officer at AMRL and has a B.Sc. (Hons) in Metallurgy from the UNSW and a M.Sc. in Mathematics from the University of Melbourne and is curently a member of the Australian Composites Structures Society. He joined AMRL in 1986 and has worked on the materials science of adhesives and composite materials.

L. R. F. Rose
Airframes and Engines Division

Francis Rose graduated with a B.Sc (Hons.) from the University of Sydney in 1971 and a Ph.D from Sheffield University, UK in 1975.
He was appointed as a Research Scientist at the Aeronautical Resarch Laboratory in 1976 and is currently the Research Leader in Fracture Mechanics in the Airframes and Engines Division. He has made important research contributions in fracture mechanics, non-destructive evaluationa and applied mathematics. He is the regional Editor for the International Journal of Fracture and a member of the editorial board of Mechancis of Materials. He is also a Fellow of the Intstitute for Applied Mathematics and its Applications, UK and a Fellow of the Institute of Engineers, Australia.

Contents

1. Introduction

Bonded composite repairs are an effective and cost-efficient means of restoring the life of cracked metallic aircraft components. The Aeronautical and Maritime Research Laboratory (AMRL) has used this technique [1] for over 25 years to repair damaged Royal Australian Air Force (RAAF) aircraft. A critical step in the repair design process is to obtain an accurate estimate of the stress intensity factor associated with the crack in the metallic component after application of the repair. In the initial design stage, analytical formulae are used to obtain these estimates.

The purpose of this paper is to assess the accuracy of the current technique and to explore other analytical techniques that might provide improved estimates. Truly conservative estimates are desirable for the initial design stage and the conservative nature of the estimates is assessed through the concept of variational bounds. Variational bounds for the equivalent spring constant of a bonded repair arise from minimising the complementary energy functional when either stress (lower bound) or displacement potentials (upper bound) are employed.

The accuracy of the various models is established by comparison with finite-element analysis results that are taken as "exact". A second criterion by which the models are judged is the simplicity of the expressions obtained for the design parameters of interest. Solutions based on prescribed stress potentials that satisfy the equilibrium equations of continuum mechanics, for instance, may yield accurate values for the equivalent spring constant of the repair scheme but may be very complex to evaluate. By relaxing certain assumptions simpler but still accurate solutions may be obtained. However, the theoretical guarantee of a true lower bound is lost.

An important aspect of establishing the accuracy of the various analytical models was to consider isotropic and orthotropic adherend joints having a range of adherend thicknesses. Some models are accurate for only a small range of adherend thicknesses so it was necessary to consider a wide range adherend thicknesses.

The plan of the report is as follows: in Section 2 the double-strap joint (Figures 1 and 2), which is representative of typical bonded repairs, is described, the concept of the equivalent spring constant is summarised and the existence of variational bounds established; in Section 3 the finite-element model and results for both the isotropic and orthotropic adherend double-strap joints are tabled and in Section 4 the various analytical models and results are given along with comparison of the finite-element results. Conclusions are given in Section 5.

2. The Equivalent Spring-Constant Concept

2.1 Geometry of the Double-Strap Joint

The double-strap joint (DSJ) represents a section through the central section of a double-sided repair as shown in Figure 1. It is also representative of one-sided repairs in which there is substantial restraint against out-of-plane bending.

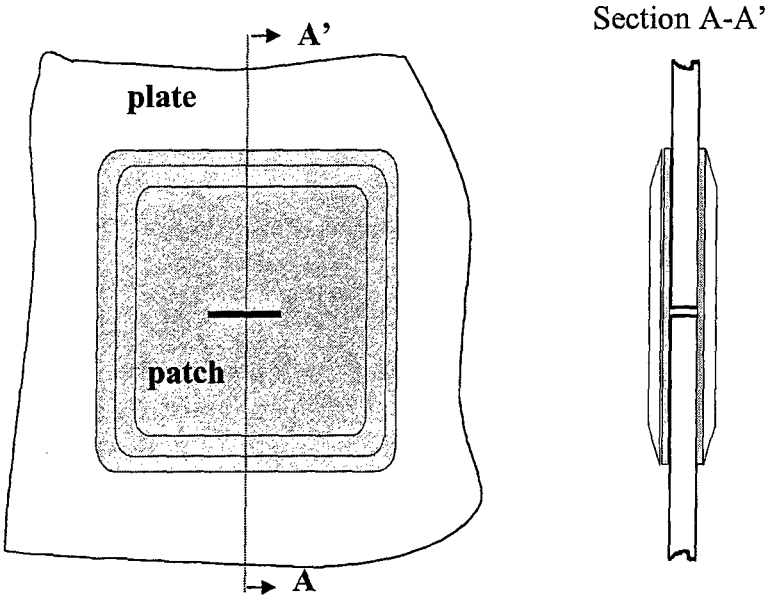

Figure 1. The DSJ as a Subelement of a Double-Sided Repair.

The nomenclature for the joint geometry is shown in Figure 2 below:

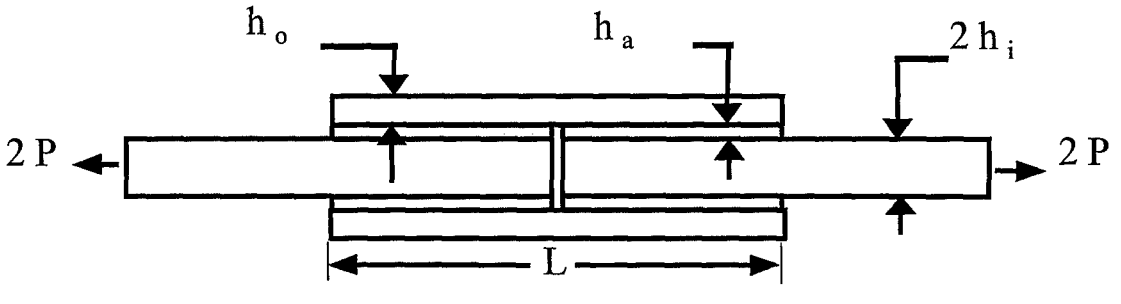

Figure 2. Nomenclature for the DSJ.

The subscripts *i*, *o* and *a* refer to the inner adherend, the outer adherend and the adhesive respectively. The material properties are similarly designated with E_i, E_o and E_a representing the Young's moduli for example.

For simplicity of mathematical modelling an infinite ($L \rightarrow \infty$) DSJ was modelled. DSJ's of sufficiently long overlap length are well approximated by such a model. A quarter model of the infinite DSJ, taking account of the symmetry of the joint across its mid-plane is shown in Figure 3.

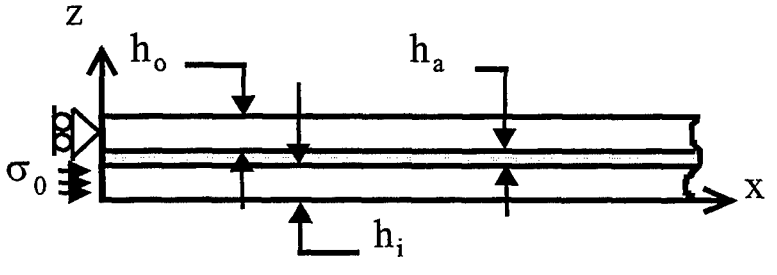

Figure 3. Quarter model of the identical adherend infinite DSJ (NB. The **z** *and* **x** *axes are axes of symmetry).*

2.2 Definition of the Equivalent Spring Constant

Rose [2] introduced the concept of an equivalent spring constant to model partial reinforcement of cracked substrates. The constraint imposed by the bonded composite repair on the opening of the crack is simulated by a distribution of springs across the crack faces. A simplified assessment of the repair efficiency arises from such an approach. The springs across the crack faces have an equivalent spring constant, *k*, which is given by:

$$\sigma_0 = E_i k \hat{u} \ , \tag{1}$$

where σ_0 is the applied stress, E_i is the Young's modulus of the inner adherend and $\hat{u}$ is the average displacement of the inner adherend in the *x* direction.

Equivalently, *k* can be defined in terms of the complementary energy, U_c [2]:

$$\begin{aligned} U_c &= \frac{1}{2}\sigma_0 \hat{u} \\ &\ldots = \frac{1}{2}\frac{\sigma_0^{\,2}}{E_i k}. \end{aligned} \tag{2}$$

The complementary energy, when the strains are expressed in terms of stresses, is also given by:

$$U_c = \Sigma_i \frac{1}{2}\sigma^i \varepsilon^i + \Sigma_o \frac{1}{2}\sigma^o \varepsilon^o + \Sigma_a \frac{1}{2}\sigma^a \varepsilon^a \tag{3}$$

where the summations are over all the stresses present in the inner adherend, outer adherend and adhesive respectively.

2.3 Variational bounds

As discussed in Hashin [3], a U_c functional associated with admissible stresses leads to a lower bound on the longitudinal Young's modulus for a cracked laminate. Similarly for the DSJ, a U_c functional associated with admissible stresses leads to a lower bound on k while a U_c functional associated with displacements leads to an upper bound k:

$$k_\sigma \leq k \leq k_u \tag{4}$$

3. Finite Element Results

The finite element (FE) package PAFEC [4] was used to model the DSJ. A plane-strain two-dimensional model (Figure 4) employing eight-noded isoparametric elements was used.

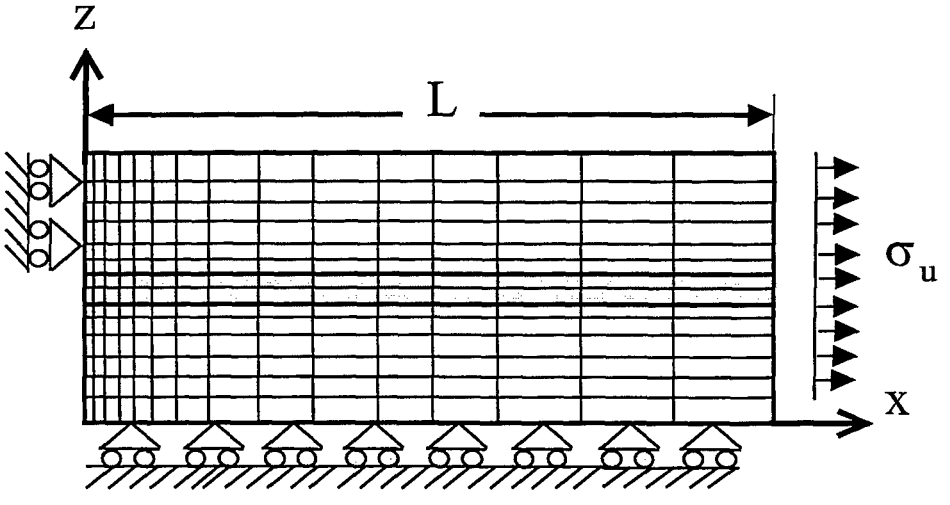

Figure 4. FE quarter-model of the DSJ showing loading and constraints.

The following linear-elastic material properties were used:

adhesive

$$G_a = 700 \text{ MPa}$$
$$\nu_a = 0.35$$

isotropic adherends

$$E = 71 \text{ GPa}$$
$$\nu = 0.33$$

orthotropic adherends

$$E_L = 208.3 \text{ GPa}$$
$$E_T = 25.4 \text{ GPa}$$
$$G_{LT} = 7.24 \text{ GPa}$$
$$\nu_{LT} = 0.183$$
$$\nu_{TL} = 0.1667$$

The orthotropic material properties of a typical fibre-composite material have been simplified to those of a transversely isotropic material to simplify the analysis. The isotropic plane is taken to be the plane perpendicular to the fibre direction and only a unidirectional layup has been considered.

The following boundary conditions (see Figure 3.1) were applied to the model. A uniform stress, σ_u, was applied at the end of the joint and the longitudinal displacements there constrained to be uniform across the thickness:

$$\sigma_{xx}\left(x = L, 0 \le z \le h_i + h_a + h_o\right) = \sigma_u \tag{5}$$

$$u_x{}^i\left(x = L, 0 \le z \le h_i\right) = u_x{}^a\left(x = L, h_i < z \le h_i + h_a\right)$$
$$= u_x{}^o\left(x = L, h_i + h_a < z \le h_i + h_a + h_o\right) \tag{6}$$

where the letters *i*, *o* and *a* denote the inner adherend, the outer adherend and the adhesive respectively.

Other constraints on the displacements were:

$$u_z{}^i\left(0 \le x \le L, z = 0\right) = 0 \tag{7}$$

$$u_x^{\,o}\left(x=0, h_i+h_a<z\le h_i+h_a+h_o\right)=0 \tag{8}$$

Mesh refinement was carried out to ensure convergence of the models. Details of the mesh refinement can be found in reference [5].

The FE value of k was obtained by taking the average of the x displacements of inner adherend at $x=0$:

$$\hat{u}=\frac{1}{h_i}\int_0^{h_i} u_x^{\,i}(x=0)dz \tag{9}$$

where the integral was evaluated numerically using FE displacements and Simpson's Rule. The average was then inserted into equation 1 and k determined.

To determine the range of accuracy of the various analytical models as compared with the "exact" FE results it was first necessary to identify an appropriate measure of joint configuration variation. The measure chosen was the non-dimensional parameter α defined below:

$$\alpha=\beta_{FE}h\sqrt{\frac{E}{G}} \tag{10}$$

Two length scales comprise α. The load transfer length, β_{FE}, is a finite-element estimate of the load transfer length. The other important length scale is the St Venant length defined, for the purposes of this study, as shown below:

$$\text{St Venant Length}=h\sqrt{\frac{E}{G}} \tag{11}$$

Further details on β and the St Venant lengyth can be found in reference 5.

3.1 FE Results for the Isotropic Adherend Joints

FE results for a range of isotropic adherend DSJs having identical adherends is presented in Table 1.

*Table 1. FE Values of **k** and α for the Isotropic **DSJs**.*

h (mm)	α	k (mm^{-1})
1	0.4818	0.1303
2	0.6618	0.0887
3	0.7853	0.0698
4	0.8822	0.0585
5	0.9625	0.0507
6	1.0289	0.0449
7	1.0862	0.0405
8	1.1358	0.0368
9	1.1780	0.0339
10	1.2127	0.0314

3.2 FE Results for the Orthotropic Adherend Joints

FE results for a range of orthotropic adherend DSJs having identical adherends is presented in Table 2.

Table 2. FE Values of the $\mathbf{k}$ *and* α *for the Orthotropic DSJs.*

h (mm)	α	k (mm^{-1})
0.5	0.6526	0.1253
0.6	0.7069	0.1135
0.7	0.7564	0.1042
0.8	0.8031	0.0966
0.9	0.8447	0.0903
1.0	0.8828	0.0851
2.0	1.1803	0.0559
3.0	1.3379	0.0428
4.0	1.4708	0.0351
5.0	1.6080	0.0300

4. Analytical Models

An exact analysis of the stress state in a DSJ in which both the equilibrium equations and the compatibility equations of continuum mechanics are satisfied for all three layers and for which continuity of tractions and displacements is enforced is prohibitively complicated. Consequently, simplifying assumptions are made in formulating an analytical approach. A trade off between simplicity and accuracy is usually necessary in any approach.

The one-dimensional analytical models of the stress distribution in DSJs considered here fall broadly into two categories:

(i) Those that start from a prescribed form for the displacements and in which displacement potentials are introduced. Strains are derived from the displacements from kinematic relationships and automatically satisfy the compatibility equations of continuum mechanics. The stress-strain relations are applied to determine the stresses, statical equilibrium enforced by minimising the resulting potential energy and the result is coupled ordinary-differential equations for the adhesive stresses. These equations can be solved for the adhesive shear and peel stresses.

(ii) Those that start from a prescribed form for the some of the stress components in which stress potentials are introduced. The pointwise equilibrium equations of continuum mechanics are applied to determine the remaining stress components. The unknown coefficients are determined by minimising the complementary energy which ensures global compatability. The complementary energy is expressed in terms of the stresses and the resulting functional is minimised to yield the Euler-Lagrange equations. Coupled differential equations are again the result and these are solved for the adhesive shear and peel stresses.

The models described above yield variational bounds for $\boldsymbol{k}$. A further simplification of the analysis results if the condition of constrained elasticity is assumed [6]. Such an assumption in this context implies that for the strains in the z direction:

$$\varepsilon_z^{\,i} = \varepsilon_z^{\,o} = \varepsilon_z^{\,a} = 0 \tag{12}$$

and furthermore for the z displacements:

$$w_z^{\,i} = w_z^{\,o} = w_z^{\,a} = 0 \tag{13}$$

Consequently, stress σ_z if it exists will not contribute to the energy functional as the ε_z strain is zero.

4.1 Models That Yield Variational Bounds

4.1.1 Upper Bounds -The Prescribed Displacement Models

4.1.1.1 Hart-Smith

Hart-Smith's model is a based on simple plate theory and assumes that the deformation state in the adherends is one of simple stretching [7]. The critical assumptions are:

1) That the adherends deform purely by uniaxial tension or compression, ie, no bending, so that the only components of displacement in the adherends are:

$$u_x{}^o(x) \text{ and } u_x{}^i(x) \tag{14}$$

2) The adhesive deforms purely by shear and the strain is constrained to be:

$$\gamma(x)=\frac{1}{h_a}\left(u_x{}^o(x)-u_x{}^i(x)\right) \tag{15}$$

The complementary energy of the bonded joint becomes

$$\begin{aligned} U_c &= \int\int\left(\Sigma_i \frac{1}{2}\sigma^i\varepsilon^i+\Sigma_o\frac{1}{2}\sigma^o\varepsilon^o+\Sigma_a\frac{1}{2}\sigma^a\varepsilon^a\right)dz\,dx \\ &= \int\left(\frac{h_i}{2}E_i\left(\frac{du_x{}^i}{dx}\right)^2+\frac{h_o}{2}E_o\left(\frac{du_x{}^o}{dx}\right)^2+\frac{h_a}{2}G_a\left(\gamma_a\right)^2\right)dx. \end{aligned} \tag{16}$$

U_c is to be minimised over the range of admissible displacement functions subject to the constraint given by equation 4.1.1.1.2. A Lagrange multiplier, λ, can be used and the following equation minimised:

$$U_1\left(u_x{}^i,u_x{}^o,\gamma_a\right)=U_c\left(u_x{}^i,u_x{}^o,\gamma_a\right)+\lambda\left(\gamma_a-\frac{1}{h_a}\left(u_x{}^o-u_x{}^i\right)\right). \tag{17}$$

This leads to the set of equations:

$$\frac{\lambda}{h_a} - E_i h_i \frac{d^2 u_x{}^i}{dx^2} = 0, \frac{\lambda}{h_a} - E_i h_i \frac{d^2 u_x{}^i}{dx^2} = 0, \lambda + G_a h_a \gamma_a = 0. \tag{18}$$

The first two equations can be rearranged and subtracted to yield:

$$\lambda = \left(\frac{d^2 u_x{}^i}{dx^2} - \frac{d^2 u_x{}^o}{dx^2} \right) \frac{h_a}{\left(\frac{1}{E_o h_o} + \frac{1}{E_i h_i} \right)}. \tag{19}$$

Substitution of equation 19 into the last equation of equation set 18 yields:

$$\left(\frac{d^2 u_x{}^i}{dx^2} - \frac{d^2 u_x{}^o}{dx^2} \right) \frac{h_a}{\left(\frac{1}{E_o h_o} + \frac{1}{E_i h_i} \right)} + G_a h_a \gamma_a = 0. \tag{20}$$

Taking the second derivative of equation 15 and substituting into equation 20 gives:

$$-h_a \frac{d^2 \gamma_a}{dx^2} \frac{h_a}{\left(\frac{1}{E_o h_o} + \frac{1}{E_i h_i} \right)} + G_a h_a \gamma_a = 0. \tag{21}$$

This can be rearranged into the form given by Hart-Smith's [7] form:

$$\frac{d^2 \gamma_a}{dx^2} - \frac{G_a}{h_a} \left(\frac{1}{E_o h_o} + \frac{1}{E_i h_i} \right) \gamma_a = 0. \tag{22}$$

Thus minimising the complementary energy gives the same resulting differential equation and as imposing statical equilibrium (Hart-Smith).

The solution of which over the semi-infinite domain is:

$$\gamma_a(x) = \gamma_0 e^{-\beta x}, \tag{23}$$

where

$$\beta^2 = \frac{G_a}{h_a}\left(\frac{1}{E_o h_o} + \frac{1}{E_i h_i}\right). \quad (24)$$

The constant γ_0 is obtained by recognising that load transfer occurs purely by shear of the adhesive and that the load transferred equals $\sigma_0 h$ (in this case of identical adherends):

$$\int_0^\infty G_a \gamma_a(x) = \sigma_0 h, \quad (25)$$

Equation 23 becomes:

$$\gamma_a(x) = \frac{\sigma_0 h \beta}{G_a} e^{-\beta x}. \quad (26)$$

k can be obtained form equation 1, recognising that at $x=0$:

$$u_x{}^o(0) = 0 \text{ and } u_x{}^i(0) = \hat{u} = \frac{h_a}{G_a}\sigma_0 h\beta, \quad (27)$$

so that

$$k = \frac{\sigma_0}{E_i \hat{u}} = \frac{G_a}{E_i h_i h_a \beta}. \quad (28)$$

For identical adherend joints this reduces to:

$$k = \frac{\beta}{2} \quad (29)$$

Figure 5 plots values of k determined from equation 28 for various joint configurations, confirming that the bound is an upper bound:

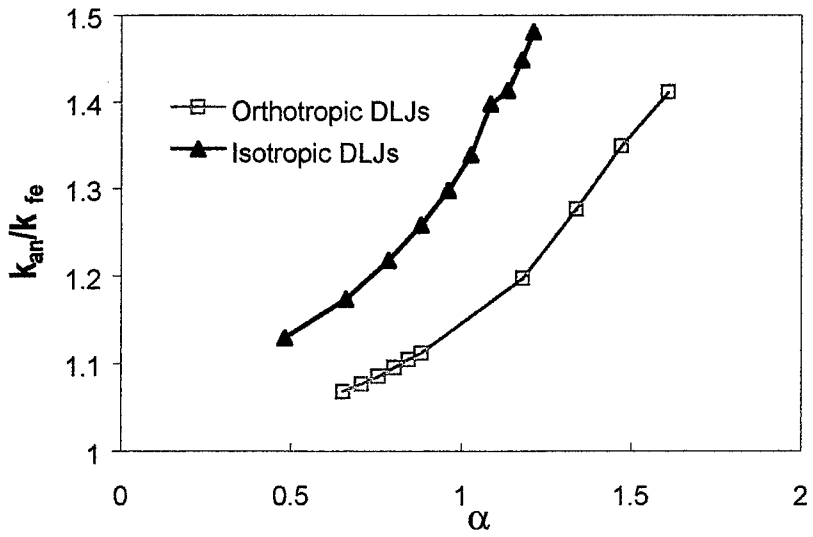

Figure 5. Plot against α of the analytical-to-FE ratio for **k** *- Hart-Smith.*

4.1.1.2 Delale, Erdogan and Aydinoglu

Delale, Erdogan and Aydinoglu's [8] model of the stresses in adhesively bonded joints applies Reissners plate theory to the adherends. The adherends are allowed to undergo bending and transverse shear. Strains in the adhesive are assumed to be constant across the thickness of the bondline.

The displacements u_x, u_z and the rotation β for the two adherends are prescribed in terms of traction, shear force and bending moment. Equations of statical equilibrium relate the traction, shear force and bending moment to the adhesive shear and peel stress.

Delale et al derived the following coupled differential equations:

$$\frac{d^3\tau_a}{dx^3}+\alpha_1\frac{d\tau_a}{dx}+\alpha_2\sigma_a=0 \tag{30}$$

$$\frac{d^4\sigma_a}{dx^4}+\beta_1\frac{d^2\sigma_a}{dx^2}+\beta_2\sigma_a+\beta_3\frac{d^3\tau_a}{dx^3}+\beta_4\frac{d\tau_a}{dx}=0. \tag{31}$$

The constants are:

$$\alpha_1 = -\frac{G_a}{h_a}\left(C_1 + C_2 + \frac{(h_o + h_a)h_o}{4} D_o\right),$$

$$\alpha_2 = \frac{G_a}{h_a}\frac{h_o}{2} D_o,$$

$$\beta_1 = \frac{E_a(1-\nu_a)}{(1-\nu_a - 2\nu_a^2)}\left(\frac{\nu_a}{2(1-\nu_a)}\frac{h_o}{2} D_o - \frac{1}{h_a}\left(\frac{1}{B_i} + \frac{1}{B_o}\right)\right),$$

$$\beta_2 = \frac{E_a(1-\nu_a)}{(1-\nu_a - 2\nu_a^2)}\frac{D_o}{h_a},$$

$$\beta_3 = -\frac{\nu_a E_a}{2(1-\nu_a - 2\nu_a^2)}\left(C_1 - C_2 + \frac{h_o(h_o + h_a)}{4} D_o\right),$$

$$\beta_4 = -\frac{\nu_a E_a}{2h_a(1-\nu_a - 2\nu_a^2)}(h_o + h_a) D_o,$$

where,

$$C_o = \frac{1-\nu_l\nu_t}{h_o E_l}, C_i = \frac{1-\nu_l\nu_t}{h_i E_l},$$

$$B_o = \frac{5}{6} h_o G_{lt}, B_i = \frac{5}{6} h_i G_{lt},$$

$$D_o = \frac{12(1-\nu_l\nu_t)}{E_l}.$$

The terms in those constants that relate to bending of the inner adherend (D_i=0) can be set to zero for the DSJ. The procedure for solving these coupled ordinary differential equations with constant coefficients is straightforward: reducing the two equations to one higher order equation in one of the stresses and substituting an exponential of form $e^{\lambda x}$ and solving the resulting characteristic equation for λ. However, the roots of the characteristic equations are quite complicated and messy. By numerically evaluating the constants and using the program Mathematica [9] exact solutions can be found though not in symbolic form.

Values of k for the various joints are shown in Figure 6, also indicating the expected upper bound:

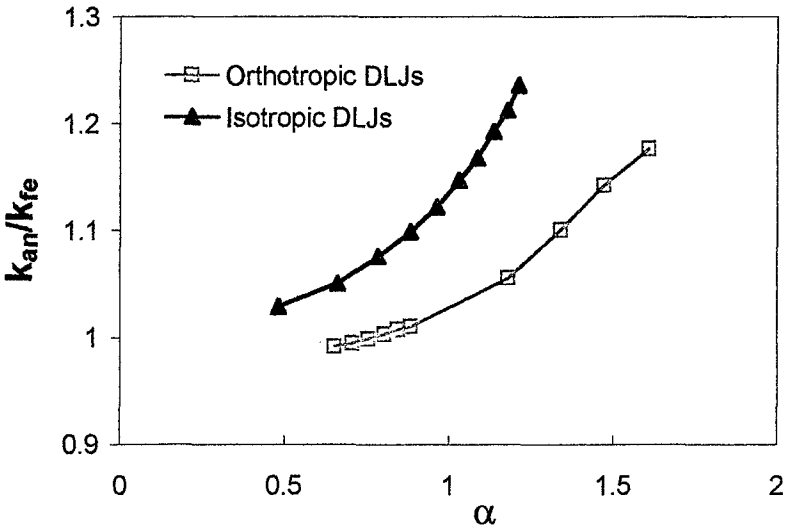

Figure 6. Plot against α of the analytical-to-FE ratio for k – *Delale* et al.

4.1.2 Lower Bounds - The Prescribed Stress Models

4.1.2.1 Hashin

The analysis developed by Hashin [3] for cracked composite laminates is extended to bonded joints in this section. Admissible stress states for the adherends and adhesive, satisfying the equilibrium equations of continuum mechanics, are developed in terms of a single stress potential, ϕ. The complementary energy of the joint is minimised to yield an ordinary differential equation in ϕ. Solution of the differential equation allows the determination of an expression for k.

The assumed stress state is:

Inner Adherend:

$$\begin{aligned} \sigma_{xx}^{\ i} &= -\sigma_0\phi(x), \\ \sigma_{zx}^{\ i} &= \sigma_0\phi'(x)z, \\ \sigma_{zz}^{\ i} &= \sigma_0\phi''(x)\frac{1}{2}\left(h_i(h_i+h_o)-z^2\right) \end{aligned} \tag{32}$$

Outer Adherend:

$$\begin{aligned}
\sigma_{xx}{}^{o} &= \sigma_0 \frac{h_i}{h_o}\phi(x), \\
\sigma_{zx}{}^{o} &= \sigma_0 \frac{h_i}{h_o}\phi'(x)\left(h_i + h_o + h_a - z\right), \\
\sigma_{zz}{}^{o} &= \sigma_0 \phi''(x)\frac{1}{2}\left(h_i + h_o + h_a - z\right)^2.
\end{aligned} \tag{33}$$

Adhesive:

$$\begin{aligned}
\sigma_{xx}{}^{a} &= 0, \\
\sigma_{zx}{}^{a} &= \sigma_0 h_i \phi'(x), \\
\sigma_{zz}{}^{a} &= \sigma_0 \frac{h_i h_o}{2}\phi''(x).
\end{aligned} \tag{34}$$

The complementary energy is given by:

$$\begin{aligned}
U_c &= \int_0^{h_i+h_o+h_a} dz \int_0^{\infty} W(x,z)dx, \\
2W &= \sum\left(\frac{\sigma_{xx}{}^2}{E_l} + \frac{\sigma_{zz}{}^2}{E_t} + \frac{\sigma_{xz}{}^2}{G} - 2\frac{\nu}{E_l}\sigma_{xx}\sigma_{zz}\right).
\end{aligned} \tag{35}$$

Contributions from the adherends and the adhesive are summed. This yields:

$$2U_c = \sigma^2 h_i{}^2 \int_0^{\infty} dx\left\{A_0\phi^2 + A_1(\phi')^2 + A_2\phi\phi'' + A_3(\phi'')^2\right\},$$

where,

$$\begin{aligned}
A_0 &= \frac{1-\left(\nu_{lt}{}^{i}\right)^2}{E_l{}^{i}h_i} + \frac{1-\left(\nu_{lt}{}^{o}\right)^2}{E_l{}^{o}h_o}, \\
A_1 &= \frac{h_a}{G_a} + \frac{h_i}{3G_{lt}{}^{i}} + \frac{h_o}{3G_{lt}{}^{o}}, \\
A_2 &= \left(\frac{1}{E_l{}^{i}} + \frac{1}{E_t{}^{i}}\right)\left(\frac{2}{3}h_i + h_o\right)\nu_{lt}{}^{i}\left(1+\nu_{tl}{}^{i}\right) - \left(\frac{1}{E_l{}^{o}} + \frac{1}{E_t{}^{o}}\right)\frac{h_o}{3}\nu_{lt}{}^{o}\left(1+\nu_{tl}{}^{o}\right), \\
A_3 &= \frac{h_i\left(1-\left(\nu_{tl}{}^{i}\right)^2\right)}{4E_t{}^{i}}\left(\frac{8}{15}h_i{}^2 + \frac{4}{3}h_ih_o + h_o{}^2\right) + \frac{h_o{}^3\left(1-\left(\nu_{tl}{}^{o}\right)^2\right)}{20E_t{}^{o}} + \frac{1}{4}h_o{}^2\frac{h_a\left(1-\nu_a{}^2\right)}{E_a}.
\end{aligned} \tag{36}$$

Minimising U_c leads to the following differential equation:

$$A_3\phi'''' + (A_2 - A_1)\phi'' + A_0 = 0. \tag{37}$$

The solution of this equation over the semi-infinite domain is:

$$\phi(x) = -\frac{\beta_2}{\beta_2 - \beta_1} e^{-\beta_1 x} + \frac{\beta_1}{\beta_2 - \beta_1} e^{-\beta_2 x}, \tag{38}$$

where the following boundary conditions have been applied:

$$-\phi(0) = 1 \text{ and } \phi'(0) = 0. \tag{39}$$

The first condition represents equation 25 and the second that the integral of the peel stress equals zero, ie:

$$\int_0^\infty \sigma_{zz}{}^a(x)dx = 0 \tag{40}$$

The constants β_1 and β_2 are given by:

$$\begin{aligned} \beta_1 &= \sqrt{\frac{1}{2A_3}}\sqrt{(A_1 - A_2) - \sqrt{(A_1 - A_2)^2 - 4A_0A_3}} \\ \beta_2 &= -\sqrt{\frac{1}{2A_3}}\sqrt{(A_1 - A_2) + \sqrt{(A_1 - A_2)^2 - 4A_0A_3}} \end{aligned} \tag{41}$$

From this solution for $\phi(x)$ the stress state for the joint is determined. k can be found by integrating the complementary energy (equation 4.3.?):

$$U_c = \frac{(\beta_1\beta_2)^2(A_1 - A_2 + A_3\beta_1\beta_2) + A_0(\beta_1{}^2 + 3\beta_1\beta_2 + \beta_2{}^2)}{2\beta_1\beta_2(\beta_1 + \beta_2)}\sigma_0 h_1{}^2 \tag{42}$$

k is then found from equation 2.

Values of k for the various joints plotted in Figure 7 below.

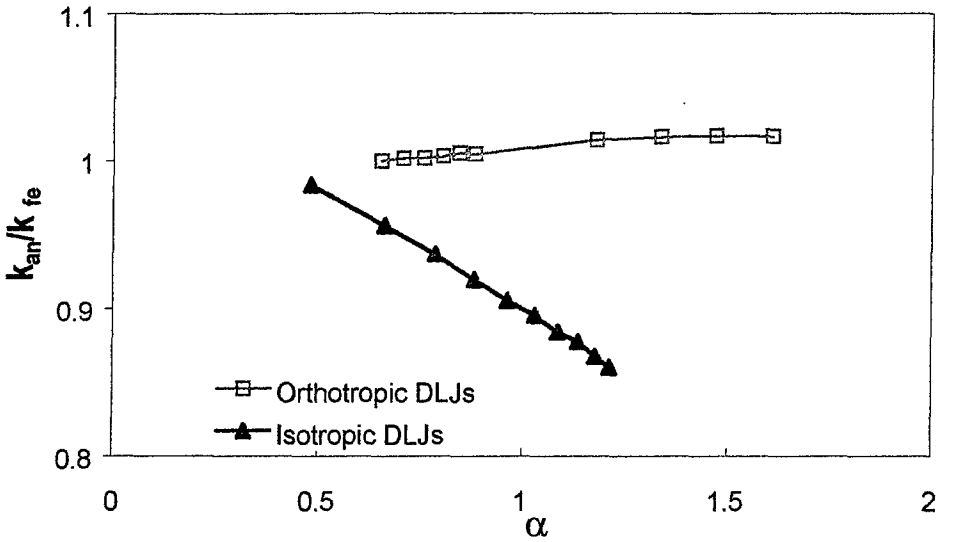

Figure 7. Plot against α of the analytical-to-FE ratio for k - *Hashin.*

4.1.2.2 Allman

Allman's analysis [10] of the double-lap joint utilises two stress potentials, $\phi_1(x)$ and $\phi_2(x)$, to describe the stress state of the joint, viz:

$$\frac{1}{2}\left(\sigma_o - \sigma_i\right) = \frac{t}{2h}\frac{\partial^2 \phi_1}{\partial x^2} \tag{43}$$

$$\frac{1}{2}\left(\sigma_o + \sigma_i\right) = \frac{\partial^2 \phi_2}{\partial x^2} \tag{44}$$

where σ_o and σ_i are the stresses normal to the bondline at the interface with the outer and inner adherend respectively.

Allman models the effects of bending, stretching and shearing of the adherends and of shearing and tearing of the adhesive layer using these two stress potentials. The advantage of two stress potentials over one is that requirement of a stress-free condition at the end of the adhesive layer can be accommodated:

$$\sigma_{zx}{}^{a}(0) = 0. \tag{45}$$

The form of the stresses in terms of stress potentials that Allman derives [10], with some modification to allow for the infinite nature of joint, for the double-lap joint is:

- for the outer adherend

$$\begin{aligned}
\sigma_{xx}^{\,o}(x) &= \frac{1}{h_o}\frac{2}{(h_o+h_i)}\left(3(1+\varepsilon_1)\eta-1\right)\phi_1(x)+\frac{6\eta\phi_2(x)}{h_o^{\,2}},\\
\tau_{xy}^{\,o}(x) &= \frac{1}{2(h_o+h_i)}\left((1+3\varepsilon_1)+2\eta-3(1+\varepsilon_1)\eta^2\right)\frac{d\phi_1}{dx}+\frac{3}{2h_o}\left(1-\eta^2\right)\frac{d\phi_2}{dx},\\
\sigma_{yy}^{\,o}(x) &= \frac{h_o}{4(h_o+h_i)}\left((1+2\varepsilon_1)-(1+3\varepsilon_1)\eta-\eta^2+(1+\varepsilon_1)\eta^3\right)\frac{d^2\phi_1}{dx^2}\\
&\quad+\frac{1}{2}\left(1-\frac{3}{2}+\frac{1}{2}\eta^3\right)\frac{d^2\phi_2}{dx^2},
\end{aligned} \tag{46}$$

  where $\eta = h_o/2$ and $\varepsilon_1=h_a/h_o$

- for the inner adherend

$$\begin{aligned}
\sigma_{xx}^{\,i} &= \frac{1}{h_i}\frac{4}{h_o+h_i}\phi_1,\\
\tau_{xy}^{\,i} &= -\frac{d\phi_1}{dx}\frac{\eta+1}{h_i+h_o},\\
\sigma_{yy}^{\,i} &= \frac{d^2\phi_2}{dx^2}-\frac{d^2\phi_1}{dx^2}\frac{1}{h_i+h_o}\left\{h_a+\frac{h_i}{4}\left(3-2\eta-\eta^2\right)\right\},
\end{aligned} \tag{47}$$

  where $\eta = h_i/2$

- for the adhesive

$$\begin{aligned}
\tau_{xy}^{\,a} &= -\frac{d\phi_1}{dx}\frac{2}{h_i+h_o},\\
\sigma_{yy}^{\,a} &= \frac{d^2\phi_2}{dx^2}+\eta\frac{h_a}{h_i+h_o}\frac{d^2\phi_1}{dx^2}.
\end{aligned} \tag{48}$$

  where $\eta = h_a/2$.

The strain energy of the joint is expressed in terms of the stress potentials and then integrated over z and x. The resulting functional is:

$$F = \int_0^{\infty} \left\{ \begin{array}{l} \alpha_1 \phi_1^{\,2} + \alpha_2 \phi_2^{\,2} + \alpha_3 \phi_1 \phi_2 + \alpha_4 \left(\phi_1^{\,I}\right)^2 + \alpha_5 \left(\phi_2^{\,I}\right)^2 \\ + \alpha_6 \left(\phi_1^{\,I} \phi_2^{\,I}\right) + \alpha_7 \left(\phi_1^{\,II}\right)^2 + \alpha_8 \left(\phi_2^{\,II}\right)^2 + \alpha_9 \phi_1^{\,II} \phi_2^{\,II} \\ + \alpha_{10} \phi_1 \phi_1^{\,II} + \alpha_{11} \phi_1 \phi_2^{\,II} + \alpha_{12} \phi_2 \phi_1^{\,II} + \alpha_{13} \phi_2 \phi_2^{\,II} \end{array} \right\} dx, \tag{49}$$

where the constants α_1 to α_{13}, for an all-isotropic adherend join, are given by:

$$\alpha_1 = \frac{1}{\left(h_i + h_o\right)^2} \left(\frac{2\left(1-\nu_i^{\,2}\right)}{E_i h_i} + \frac{\left(1-\nu_o^{\,2}\right)\left(4+6\varepsilon_1+3\varepsilon_1^{\,2}\right)}{E_o h_o} \right)$$

$$\alpha_2 = \frac{6\left(1-\nu_o^{\,2}\right)}{E_o h_o^{\,3}}$$

$$\alpha_3 = \frac{1}{\left(h_i + h_o\right)} \frac{12\left(1+\varepsilon_1\right)\left(1-\nu_o^{\,2}\right)}{E_o h_o^{\,2}}$$

$$\alpha_4 = \frac{1}{\left(h_i + h_o\right)^2} \left(\frac{2}{3}\frac{h_i}{G_i} + 2\frac{h_a}{G_a} + \frac{h_o}{15G_o}\left(4+3\varepsilon_1+9\varepsilon_1^{\,2}\right) \right)$$

$$\alpha_5 = \frac{3}{5G_o h_o}$$

$$\alpha_6 = \frac{\left(1+6\varepsilon_1\right)}{5G_o\left(h_i + h_o\right)^2}$$

$$\alpha_7 = \frac{7E_a E_o h_i \left(15ha^2 + 20h_a h_i + 8h_i^{\,2}\right)\left(1-\nu_i^{\,2}\right) - E_i\left(35E_o h_a^{\,3} - E_a h_o^{\,3}\left(4+22\varepsilon_1+39\varepsilon_1^{\,2}\right)\right)\left(1-\nu_o^{\,2}\right)}{210E_a E_i E_o\left(h_i + h_o\right)^2}$$

$$\alpha_8 = \frac{1}{2}\frac{h_i\left(1-\nu_i^{\,2}\right)}{E_i} + \frac{h_a}{2E_a} + \frac{13h_o}{70E_o}\left(1-\nu_o^{\,2}\right)$$

$$\alpha_9 = \frac{1}{105E_i E_o\left(h_i + h_o\right)} \left(E_i h_o^{\,2}\left(1-\nu_o^{\,2}\right)\left(11+39\varepsilon_1\right) - 35E_o h_i\left(3h_a + 2h_i\right) \right)$$

$$\alpha_{10} = \frac{1}{\left(h_i + h_o\right)^2} \left(\frac{2}{3}\frac{\left(3h_a + 2h_i\right)\left(1-\nu_i\right)\nu_i}{E_i} + \frac{2}{15}\frac{h_o\left(4+18\varepsilon_1+9\varepsilon_1^{\,2}\right)\left(1-\nu_i\right)\nu_i}{E_o} \right)$$

$$\alpha_{11} = \frac{1}{\left(h_i + h_o\right)} \left(\frac{\left(11+69\varepsilon_1\right)\left(1-\nu_o\right)\nu_o}{5E_o} - 2\frac{\left(1-\nu_i\right)\nu_i}{E_i} \right)$$

$$\alpha_{12} = \frac{1}{(h_i + h_o)} \frac{(1+6\varepsilon_1)(1-\nu_o)\nu_o}{5E_o}$$

$$\alpha_{13} = \frac{6(1-\nu_o)\nu_o}{5E_o h_o}$$

which is minimised to yield Euler-Lagrange equations for the two potentials. These coupled differntial equations are of the form:

$$2(\alpha_1 + (\alpha_{10} - \alpha_4)D^2 + \alpha_7 D^4)\phi_1 + (\alpha_3 + (\alpha_{11} + \alpha_{12} - \alpha_6)D^2 + \alpha_9 D^4)\phi_2 = 0 \quad (50)$$

and,

$$(\alpha_3 + (\alpha_{11} + \alpha_{12} - \alpha_6)D^2 + \alpha_9 D^4)\phi_1 + 2(\alpha_2 + (\alpha_{13} - \alpha_5)D^2 + \alpha_8 D^4)\phi_2 = 0 \quad (51)$$

These equations can be combined to give the following eigth-order differential equation for ϕ_2:

$$\beta_1\phi_2 + \beta_2 \frac{d^2\phi_2}{dx^2} + \beta_3 \frac{d^4\phi_2}{dx^4} + \beta_4 \frac{d^6\phi_2}{dx^6} + \beta_5 \frac{d^8\phi_2}{dx^8} = 0 \quad (52)$$

where β_1 to β_5 are related to α_1 to α_{13} by:

$$\beta_1 = -4\alpha_1\alpha_2 + \alpha_3^2$$

$$\beta_2 = 4(\alpha_1(\alpha_5 - \alpha_{13}) + \alpha_2(\alpha_4 - \alpha_{10}) + \frac{1}{2}\alpha_3(\alpha_{11} + \alpha_{12} - \alpha_6))$$

$$\beta_3 = (\alpha_{11} + \alpha_{12} - \alpha_6)^2 - 4((\alpha_{10} - \alpha_4)(\alpha_{13} - \alpha_5) + \alpha_2\alpha_7 + \alpha_1\alpha_8) + 2\alpha_3\alpha_9$$

$$\beta_4 = -4\alpha_7(\alpha_{13} - \alpha_5) + 4\alpha_8(\alpha_{10} - \alpha_4) + 2\alpha_9(\alpha_{11} + \alpha_{12} - \alpha_6)$$

$$\beta_5 = -4\alpha_7\alpha_8 + \alpha_9^2$$

Equation 52 involves only derivatives of even powers and so, in effect, reduces to a fourth order differential equation. Consequently, solutions for $\phi_2[x]$ that decay to zero as x approached infinity are of the form:

$$\phi_2[x] = AE^{-x\sqrt{\lambda_1}} + BE^{-x\sqrt{\lambda_2}} + CE^{-x\sqrt{\lambda_3}} + DE^{-x\sqrt{\lambda_2}} \tag{53}$$

where the constants λ_1 to λ_4 are real roots of the quartic:

$$\beta_1 + \beta_2 u + \beta_3 u^2 + \beta_4 u^3 + \beta_5 u^4 = 0 \tag{54}$$

The roots λ_1 to λ_4 all had positive real parts for the joint parameters investigated. Typically, λ_1 to λ_4 are real and λ_4 and λ_4 are complex conjugates. The stress potential, $\phi_1[x]$, has the same form as $\phi_2[x]$:

$$\phi_1[x] = EE^{-x\sqrt{\lambda_1}} + FE^{-x\sqrt{\lambda_2}} + GE^{-x\sqrt{\lambda_3}} + HE^{-x\sqrt{\lambda_2}} \tag{55}$$

The constants, E, F, G and H are related to A, B, C and D by:

$$E = A\frac{\alpha_3 + (\alpha_{11} + \alpha_{12} - \alpha_6)\lambda_1 + \alpha_9\lambda_1^{\,2}}{2(\alpha_1 + (\alpha_{10} - \alpha_4)\lambda_1 + \alpha_7\lambda_1)} \tag{56}$$

$$F = B\frac{\alpha_3 + (\alpha_{11} + \alpha_{12} - \alpha_6)\lambda_2 + \alpha_9\lambda_2^{\,2}}{2(\alpha_1 + (\alpha_{10} - \alpha_4)\lambda_2 + \alpha_7\lambda_2)} \tag{57}$$

$$G = C\frac{\alpha_3 + (\alpha_{11} + \alpha_{12} - \alpha_6)\lambda_3 + \alpha_9\lambda_3^{\,2}}{2(\alpha_1 + (\alpha_{10} - \alpha_4)\lambda_3 + \alpha_7\lambda_3)} \tag{58}$$

$$H = D\frac{\alpha_3 + (\alpha_{11} + \alpha_{12} - \alpha_6)\lambda_4 + \alpha_9\lambda_4^{\,2}}{2(\alpha_1 + (\alpha_{10} - \alpha_4)\lambda_4 + \alpha_7\lambda_4)} \tag{59}$$

The boundary conditions applied to the two stress potentials were that:

$$\tau_{xy}{}^{a}(0) = 0 \Rightarrow \frac{d\phi_1}{dx}[0] = = 0 \tag{60}$$

$$V_o(x) \to 0 \text{ as } x \to \infty \Rightarrow \frac{d\phi_2}{dx}[0] = = 0 \tag{61}$$

$$\int_0^\infty \tau_{xy}{}^{a}(x)dx = -F \Rightarrow \phi_1[0] = -F\frac{h_i + h_o}{2} \tag{62}$$

$$M_o(x) \to 0 \text{ as } x \to \infty \Rightarrow \frac{d\phi_2}{dx}[0] = = 0 \tag{63}$$

where M_o and V_o are the bending moment and shear force resultants in the outer adherend respectively.

Once the two stress potentials are determined k can be found by integrating U_c directly via equation 2.

The results are shown in Figure 8 for the two types of joints.

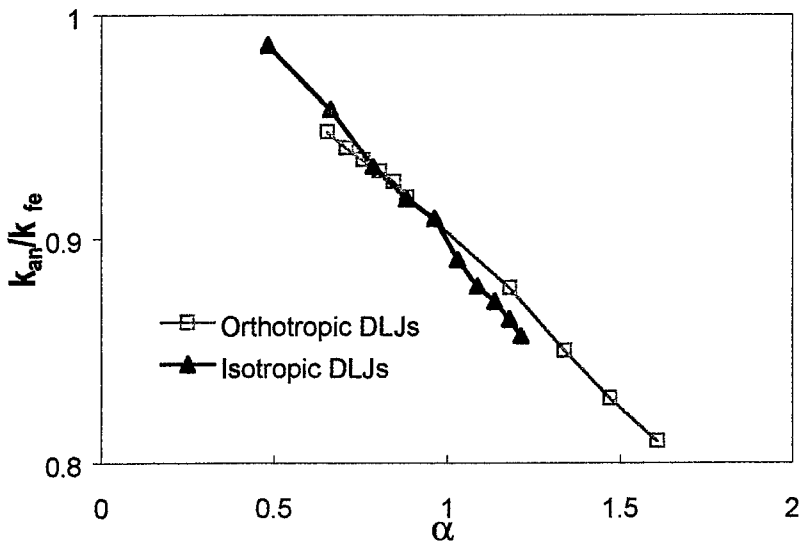

Figure 8. Plot against α of the analytical-to-FE ratio for k - *Allman.*

4.2 Constrained Elasticity Models

The constrained elasticity models impose the additional constraint (transverse-inextensibilty) that:

$$\varepsilon_z = 0 \ . \tag{64}$$

Constrained elasticity models have been used successfully by Savoia and Tullini [11] to derive a beam theory for strongly orthotropic materials. This approach can be used when the height of the beam is sufficiently small with repsect to the length or when the Young's modulus. The stress tensor then divides into an active and a reactive part. The reactive part, σ_{zz}, does no work for any admissible deformation.

For bonded joints, which are typically long and slender and often have orthotropic adherends, transverse inextensibility applies to both adherends:

$$u^{i,o}{}_{z,z} = 0 \Rightarrow u^{i,o}{}_{z}(x,z) = v^{i,o}(x). \tag{65}$$

Symmetry imposes the following boundary condition:

$$u^{i}{}_{z}(x,0) = v^{i}(x) = 0. \tag{66}$$

Within the constrained elasticity format it is possible to prescribe the format of either the displacements or the stresses. The guarantee of true upper or lower bounds is lost however. These two approaches are described below.

4.2.1 Prescribed Displacement Model

The form of the displacements in the adherends can be specified using the polynomial form adopted by Savoia and Tullini [11]:

$$u^{i}{}_{x}(x,\zeta) = \sum_{0} P_{2n}(\xi)\Phi_{2n}(x),, \tag{67}$$

where $\xi = 2z/h_i$.

The polynomials P_{2n} are defined by a recurrence relation:

$$P_0 = 1,\ P_1 = \xi, \frac{d^2 P_n}{d\xi^2} = -P_{n-2} \text{ for n} \geq 2. \tag{68}$$

P_n also has the useful property that:

$$\int_{-1}^{1} P_n d\xi = \int_{-1}^{1} \xi P_n d\xi = 0 \text{ for n} \geq 2. \tag{69}$$

This leads to the interpretation of $\Phi_0(\xi)$ as the thickness-averaged value of $u^i{}_x$.

A solution to order P_2 can be obtained as follows. For the inner adherend the displacements are:

$$\begin{aligned} u^{i}{}_{x}(x,\xi) &= u^{i}(x) + P_1(\xi)\Phi^{i}{}_{1}(x) + P_2(\xi)\Phi^{i}{}_{2}(x) \\ &= u^{i}(x) + \xi\Phi^{i}{}_{1}(x) + \frac{(1-3\xi^2)}{6}\Phi^{i}{}_{2}(x), \\ u^{i}{}_{z}(x,\xi) &= 0. \end{aligned} \tag{70}$$

The shear stress in the adherend is then:

$$\begin{aligned}\sigma^{i}{}_{x\xi}(x,\xi) &= G_i \frac{d\xi}{dz}\left(P_1'(\xi)\Phi^{i}{}_1(x) + P_2'(\xi)\Phi^{i}{}_2(x)\right) \\ &= G_i \frac{d\xi}{dz}\left(\Phi^{i}{}_1(x) - \xi\Phi^{i}{}_2(x)\right).\end{aligned} \tag{71}$$

The boundary condition on the inner adherend shear stress is:

$$\sigma^{i}{}_{x\xi}(x,\xi=\pm 1) = \pm\tau(x), \tag{72}$$

which implies,

$$\Phi^{i}{}_2(x) = -\frac{h_i}{G_i}\tau(x) \text{ and } \Phi^{i}{}_1(x) = 0. \tag{73}$$

So that,

$$u^{i}{}_x(x,\xi) = u^{i}(x) - \frac{h_i}{G_i}\frac{\left(1-3\xi^2\right)}{6}\tau(x), \tag{74}$$

Similarly, for the outer adherend:

$$\begin{aligned}u^{o}{}_x(x,\xi) &= u^{o}(x) + P_1(\xi)\Phi^{o}{}_1(x) + P_2(\xi)\Phi^{o}{}_2(x) \\ &= u^{o}(x) + \xi\Phi^{o}{}_1(x) + \frac{\left(1-3\xi^2\right)}{6}\Phi^{o}{}_2(x).\end{aligned} \tag{75}$$

The boundary condition on the outer adherend shear stress is:

$$\sigma^{i}{}_{x\xi}(x,\xi=\pm 1) = \mp\tau(x). \tag{76}$$

So that,

$$\begin{aligned}&\Phi^{o}{}_2(x) = -\frac{h_o}{G_o}\tau(x) \text{ and } \Phi^{o}{}_1(x) = 0, \\ &u^{o}{}_x(x,\xi) = u^{o}(x) + \frac{h_o}{G_o}\frac{\left(1-3\xi^2\right)}{6}\tau(x).\end{aligned} \tag{77}$$

As for the Hart-Smith analysis, the complementary energy of the bonded joint becomes

$$U_c = \int\int\left(\sum_i \frac{1}{2}\sigma^i\varepsilon^i + \sum_o \frac{1}{2}\sigma^o\varepsilon^o + \sum_a \frac{1}{2}\sigma^a\varepsilon^a\right)dz\,dx$$

$$= \int\left(\frac{h_i}{2}E_i\left(\frac{du_x{}^i}{dx}\right)^2 + \frac{h_o}{2}E_o\left(\frac{du_x{}^o}{dx}\right)^2 + \frac{h_a}{2}G_a\left(\gamma_a\right)^2\right)dx \tag{78}$$

U_c is to be minimised over the range of admissible displacement functions subject to the constraint given by equation

$$\begin{aligned}\gamma(x) &= \frac{1}{h_a}\left(u_x{}^o(x,\xi=-1) - u_x{}^i(x,\xi=1)\right)\\ &= \frac{1}{h_a}\left(u^o - u^i - \frac{\tau}{3}\left(\frac{h_i}{G_i}+\frac{h_o}{G_o}\right)\right)\\ &= \left(u^o - u^i\right)\frac{1}{G_a\left(\frac{h_a}{G_a}+\frac{h_i}{G_i}+\frac{h_o}{G_o}\right)}.\end{aligned} \tag{79}$$

A Lagrange multiplier, λ, can be used and the following equation minimised:

$$U_1\left(u_x{}^i, u_x{}^o, \gamma_a\right) = U_c\left(u_x{}^i, u_x{}^o, \gamma_a\right) + \lambda\left(\gamma_a - \frac{1}{G_a\left(\frac{h_a}{G_a}+\frac{h_i}{G_i}+\frac{h_o}{G_o}\right)}\left(u^o - u^i\right)\right) \tag{80}$$

This leads to the set of equations:

$$\frac{\lambda}{h_a} - E_i h_i \frac{d^2 u_x{}^i}{dx^2} = 0,\ \frac{\lambda}{h_a} - E_i h_i \frac{d^2 u_x{}^i}{dx^2} = 0,\ \lambda + G_a h_a \gamma_a = 0. \tag{81}$$

These equations can be solved to yield solutions for the displacements. k can be determined from the same approach as used in the Hart-Smith analysis.

Figure 9 plots values of k determined from equation 2 for various joint configurations:

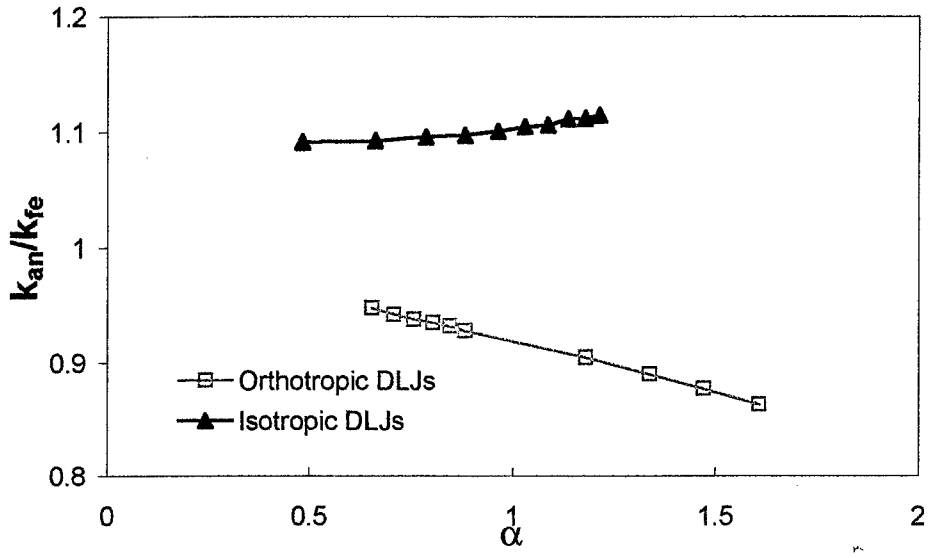

Figure 9. Plot against α of the analytical-to-FE ratio for k - *S&V/Rose.*

4.2.2 Prescribed Stress Models

Prescribed stress models can also be developed within the constrained elasticity framework. Two models are developed – one that models adherends tractions only and one that models tractions and moments.

A slighlty different nomenclature is used in the following two models: the inner adherend thickness is taken as h_i rather than $2h_i$ as previously.

4.2.2.1 Tractions Model

The adherend stresses are defined in terms of inner adherend traction, N_i, and the outer adherend traction, N_o:

$$\sigma^{i}{}_{x}(x) = \frac{N_i(x)}{h_i}, \qquad \sigma^{o}{}_{x}(x) = \frac{N_o(x)}{h_o}. \tag{82}$$

The other active stresses are determined from the equilibrium equations:

$$\begin{aligned}\sigma^{i}{}_{xz}(x,z_i) &= -2z_i\frac{N_i^{'}(x)}{h_i},\\ \sigma^{o}{}_{xz}(x,z_o) &= N_o^{'}(x)\left(\frac{1}{2}-\frac{z_o}{h_o}\right),\end{aligned} \tag{83}$$

where z_i and z_o are coordinate systems local to the inner and outer adherends respectively.

The boundary conditions are:

$$\begin{aligned}&\sigma^{i}{}_{xz}(x,h_i/2) = -N_i^{'}(x),\\ &\sigma^{i}{}_{xz}(x,0) = 0,\\ &\sigma^{o}{}_{xz}(x,-h_o/2) = N_o^{'}(x),\\ &\sigma^{o}{}_{xz}(x,+h_o/2) = 0,\end{aligned} \tag{84}$$

The complementary energy, equation 3, is constructed and minimised and the resulting Euler-Lagrange equations solved to give:

$$\gamma_a(x) = \gamma_0 e^{-\beta x}, \tag{85}$$

where, for an orthotropic material:

$$\beta^2 = \left(\frac{2\left(1 - \nu_{lt}^{\,o}\nu_{tl}^{\,o}\right)}{E_l^{\,o} h_o} + \frac{\left(1 - \nu_{lt}^{\,i}\nu_{tl}^{\,i}\right)}{E_l^{\,i} h_i} \right)\left(\frac{h_a}{G_a} + \frac{h_i}{6G_{lt}^{\,i}} + \frac{h_o}{3G_{lt}^{\,o}} \right)^{-1}. \tag{86}$$

k is given by equation 29 for an identical adherend joint. Plots of k are shown in Figure 10 below.

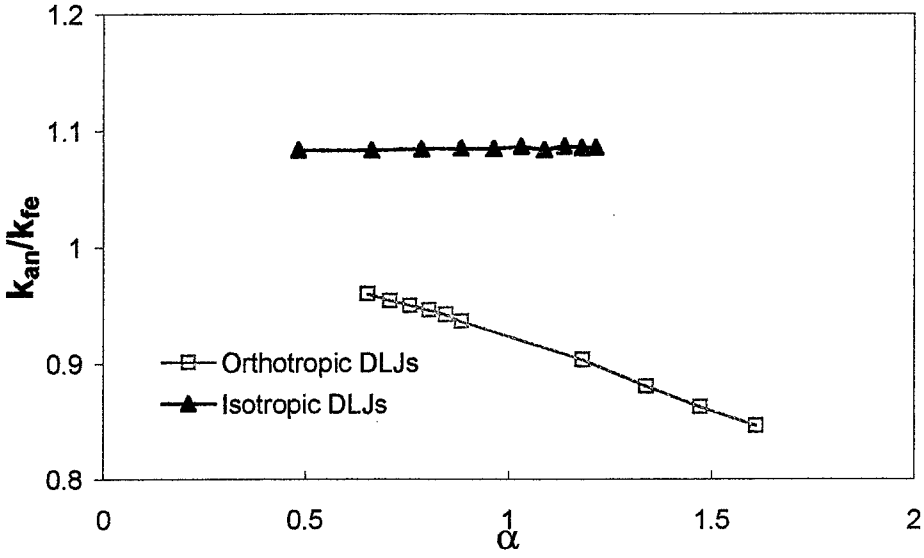

Figure 10. Plot against α of the analytical-to-FE ratio for k - S&V/Rose.

4.2.2.2 Tractions And Moments Model

The adherend stresses can be defined in terms of tractions and moments:

$$\begin{aligned} \sigma^{i}{}_{x}(x) &= \frac{N_i(x)}{h_i}, \\ \sigma^{o}{}_{x}(x) &= \frac{N_o(x)}{h_o} + M_o(x)\frac{z_o}{I_o}. \end{aligned} \tag{87}$$

The other active stresses are determined from the equilibrium equations:

$$\sigma^{i}{}_{xz}(x,z_i) = -2z_i \frac{N_i'(x)}{h_i},$$

$$\sigma^{o}{}_{xz}(x,z_o) = N_o'(x)\left(\frac{1}{2} - \frac{z_o}{h_o}\right) + M_o'(x)\frac{\left(\frac{h_o^2}{4} - z_o^2\right)}{2I_o} \tag{88}$$

The boundary conditions, equations 84, are satisfied by these equations.

The complementary energy, equation 3, is minimised and the resulting Euler-Lagrange equations solved. The resulting expressions were very complicated. By numerically evaluating the constants and using the program Mathematica exact solutions were found though not in symbolic form.

k can be determined from integrating the complementary energy. Plots of k are shown in Figure 11 below.

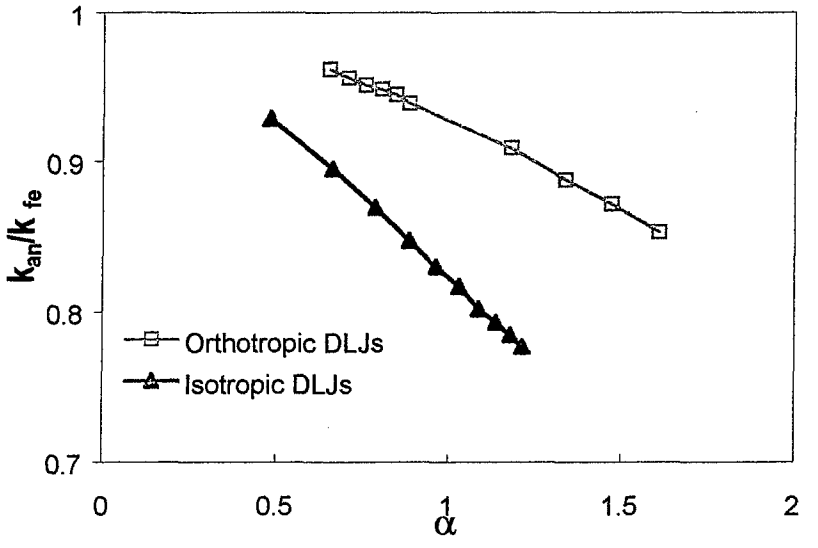

Figure 11. Plot against α of the analytical-to-FE ratio for k - *S&V/Rose.*

5. Discussion and Conclusions

Expressions that yield variational bounds for the equivalent spring constant of the double-strap joint have been obtained. These expressions should be useful in obtaining more exact estimates of the stress intensity factor associated with patched cracks.

True upper bounds were obtained from the Hart-Smith and Delale *et al* displacement based models. The Hart-Smith model is used in RAAF Engineeering Standard C5033 and gave the least conservative results. Delale's model gives improved results but is a mathematically complicated formulation.

True lower bounds for the equivalent spring constant, which are useful for obtaining truly conservative estimates for patched cracks, were obtained from the Allman and Hashin stress-based models. The Hashin model was more accurate for the joints considered, especially for orthotropic joints.

The constrained elasticity models worked quite well although the guarantee of true upper or lower bounds was lost. However, the tractions and moments model gave conservative results over the range of joints considered.

The Hashin model was the probably the best model considered – it gave truly conservative estimates of k, was reasonably accurate over a wide range of joint parameters and an analytical expression was obtained for k.

6. References

1. A. A. Baker, "Crack Patching: Experimental Studies, Practical Applications", Chapter 6 in "Bonded Repair of Aircraft Structures", Ed. By A. A. Baker and R. Jones, Martinus Nijhoff Publishers, Dordrecht, 1988.

2. L. F. R. Rose, "Theoretical Analysis of Crack Patching", Chapter 5 in "Bonded Repair of Aircraft Structures", Ed. By A. A. Baker and R. Jones, Martinus Nijhoff Publishers, Dordrecht, 1988.

3. Z. Hashin, "Analysis of Orthogonally Cracked Laminates Under Tension", Transactions of the ASME, Vol. 54, December 1987.

4. PAFEC Ltd., Strelley Hall, Nottingham, NG8 6PE, UK.

5. P. D. Chalkley and L. R. F. Rose, "A Critical Review of Some Select One-Dimensional Analytical Models of Elastic Stresses in Double Strap Joints", CRC-ACS TM 97008.

6. M. Savoia and N. Tullini, "Beam Theory for Strongly Orthotropic Materials", Int J. Solids Structures", vol. 33, No. 17, pp 2459-2484, 1996.

7. L. J. Hart-Smith, "Adhesive-Bonded Double-Lap Joints", Douglas Aircraft Co., NASA Langley Report CR-11234, January 1973.

8. F. Delale, F. Erdogan and M. N. Aydinoglu, "Stresses in Adhesively Bonded Joints: A Closed Form Solution", J. Composite Materials, Vol. 15 (May 1981), p. 249.

9. S. Wolfram, "The Mathematica book - 3rd Edition", Wolfram Media/Cambridge University Press, 1996.

10. D. J. Allman, "A Theory for Elastic stresses in Adhesive Bonded Lap Joints", Q. Jl Mech appl. Math., Vol. XXX, Pt. 4, 1977.

11. M. Savoia and N. Tullini, "Beam theory for Strongly Orthotropic Materials", Int. J. Solids and Structures, vol. 37, no. 17, pp 2459-2484, 1996.

DISTRIBUTION LIST

Variational Bounds for the Equivalent Spring Constants for Bonded Repairs

Peter Chalkley and L. R. F. Rose

AUSTRALIA

DEFENCE ORGANISATION

Task Sponsor
ASI4-1A

S&T Program
Chief Defence Scientist
FAS Science Policy
AS Science Corporate Management
} shared copy
Director General Science Policy Development
Counsellor Defence Science, London (Doc Data Sheet)
Counsellor Defence Science, Washington (Doc Data Sheet)
Scientific Adviser to MRDC Thailand (Doc Data Sheet)
Director General Scientific Advisers and Trials/Scientific Adviser Policy and Command (shared copy)
Navy Scientific Adviser (Doc Data Sheet and distribution list only)
Scientific Adviser - Army (Doc Data Sheet and distribution list only)
Air Force Scientific Adviser
Director Trials

Aeronautical and Maritime Research Laboratory
Director

Chief of Airframes and Engines Division
RLFM, RLACS
Richard Chester – Functional Head Composites
Peter Chalkley
L. R. F. Rose

DSTO Library
Library Fishermens Bend
Library Maribyrnong
Library Salisbury (2 copies)
Australian Archives
Library, MOD, Pyrmont (Doc Data sheet only)

Capability Development Division
Director General Maritime Development (Doc Data Sheet only)
Director General Land Development (Doc Data Sheet only)
Director General C3I Development (Doc Data Sheet only)

Army
ABCA Office, G-1-34, Russell Offices, Canberra (4 copies)
SO (Science), DJFHQ(L), MILPO Enoggera, Queensland 4051 (Doc Data Sheet only)
NAPOC QWG Engineer NBCD c/- DENGRS-A, HQ Engineer Centre Liverpool Military Area, NSW 2174 (Doc Data Sheet only)

Air Force
ASI-SRS Max Davis

Intelligence Program
DGSTA Defence Intelligence Organisation

Corporate Support Program (libraries)
OIC TRS, Defence Regional Library, Canberra
Officer in Charge, Document Exchange Centre (DEC) (Doc Data Sheet and distribution list only)
*US Defence Technical Information Center, 2 copies
*UK Defence Research Information Centre, 2 copies
*Canada Defence Scientific Information Service, 1 copy
*NZ Defence Information Centre, 1 copy
National Library of Australia, 1 copy

UNIVERSITIES AND COLLEGES
Australian Defence Force Academy
Library
Head of Aerospace and Mechanical Engineering
Deakin University, Serials Section (M list), Deakin University Library, Geelong, 3217
Senior Librarian, Hargrave Library, Monash University
Librarian, Flinders University

OTHER ORGANISATIONS
NASA (Canberra)
AGPS

OUTSIDE AUSTRALIA

ABSTRACTING AND INFORMATION ORGANISATIONS
INSPEC: Acquisitions Section Institution of Electrical Engineers
Library, Chemical Abstracts Reference Service
Engineering Societies Library, US
Materials Information, Cambridge Scientific Abstracts, US
Documents Librarian, The Center for Research Libraries, US

INFORMATION EXCHANGE AGREEMENT PARTNERS
Acquisitions Unit, Science Reference and Information Service, UK
Library - Exchange Desk, National Institute of Standards and Technology, US
National Aerospace Laboratory, Japan
National Aerospace Laboratory, Netherlands

SPARES (5 copies)

Total number of copies: 54

DEFENCE SCIENCE AND TECHNOLOGY ORGANISATION
DOCUMENT CONTROL DATA

1. PRIVACY MARKING/CAVEAT (OF DOCUMENT)

2. TITLE

Variational Bounds for the Equivalent Spring Constants for Bonded Repairs

3. SECURITY CLASSIFICATION (FOR UNCLASSIFIED REPORTS THAT ARE LIMITED RELEASE USE (L) NEXT TO DOCUMENT CLASSIFICATION)

Document	(U)
Title	(U)
Abstract	(U)

4. AUTHOR(S)

Peter Chalkley and L. R. F. Rose

5. CORPORATE AUTHOR

Aeronautical and Maritime Research Laboratory
PO Box 4331
Melbourne Vic 3001 Australia

6a. DSTO NUMBER	6b. AR NUMBER	6c. TYPE OF REPORT	7. DOCUMENT DATE
DSTO-RR-0139	AR-010-644	Research Report	September 1998

8. FILE NUMBER	9. TASK NUMBER	10. TASK SPONSOR	11. NO. OF PAGES	12. NO. OF REFERENCES
M1/9/504	98/188	RAAF ASI-1A	33	11

13. DOWNGRADING/DELIMITING INSTRUCTIONS

14. RELEASE AUTHORITY

Chief, Airframes and Engines Division

15. SECONDARY RELEASE STATEMENT OF THIS DOCUMENT

Approved for public release

OVERSEAS ENQUIRIES OUTSIDE STATED LIMITATIONS SHOULD BE REFERRED THROUGH DOCUMENT EXCHANGE CENTRE, DIS NETWORK OFFICE, DEPT OF DEFENCE, CAMPBELL PARK OFFICES, CANBERRA ACT 2600

16. DELIBERATE ANNOUNCEMENT

No Limitations

17. CASUAL ANNOUNCEMENT Yes

18. DEFTEST DESCRIPTORS

Bonded Composite Repairs, Military Aircraft, Cracks, Joints

19. ABSTRACT

Variational bounds, both upper and lower, are found for the equivalent spring constant of a double-strap joint which represents a sub-element of bonded repairs to cracked structure. Conservative estimates of the equivalent spring constant, needed for accurate design, are obtained from variational analyses of the joint. Estimates from various analytical models of varying level of approximation were obtained. Simpler expressions for the spring constant resulted from relaxing certain assumptions, however, the theoretical guarantee of a true upper or lower bound was lost. Spring constant estimates were compared with finite-element model results and so the fidelity of the variational bounds, specially for the simplified analyses, could be established. An improved formula is proposed for use in design procedures in RAAF C5033.